Geometry and scaling relations of a population of very small rift-related normal faults

Roy W. Schlische
Scott S. Young
Rolf V. Ackermann
Department of Geological Sciences, Rutgers University, Busch Campus, Piscataway, New Jersey 08855-1179
Anupma Gupta
Department of Geological Sciences and Lamont-Doherty Earth Observatory of Columbia University, Palisades, New York 10964

ABSTRACT

Exceptionally well exposed normal faults within the Solite Quarry of the Dan River rift basin range in length from a few millimetres to a few metres and are possibly the smallest visible faults studied to date. Displacement is greatest at or near the center of isolated faults and decreases toward the fault tips. Relay structures form between closely overlapping faults. The distribution of fault sizes in the study area follows a power-law (fractal) relation, and the maximum observed displacement scales linearly with fault length. The new fault data extend the global data set to more than eight orders of magnitude of fault length and indicate that there is no significant change in displacement geometry and the linear length-displacement scaling relation between small and large faults.

INTRODUCTION

Fault populations have been the subject of considerable study within the past decade. Most work has focused on deciphering the scaling relations of fault populations, including the size distribution of faults, the relationship between displacement and length, and the strain accommodated by faulting. Many fault populations exhibit a power-law distribution of fault sizes (e.g., Pickering et al., 1995); current debate focuses on the range of sizes over which a power-law distribution holds and the relative contribution of small and large faults to strain (e.g., Scholz and Cowie, 1990; Marrett and Allmendinger, 1991; Nichol et al., 1996). It is generally agreed that the displacement-length scaling relation is given by $D = cL^n$, where D is displacement, c is a constant related to rock properties, L is length, and n is some exponent; however, the value of n is very controversial (e.g., Gillespie et al., 1992; Cowie and Scholz, 1992a).

Most research on fault populations has focused on faults with lengths >1 m and displacements >1 cm. Small faults ($L < 1$ m) offer several advantages: (1) they are commonly well exposed, (2) large numbers are present in a small area, (3) they are likely to be confined to a single lithology, and (4) the faults are small enough to be entirely contained within hand samples, thus allowing serial sectioning and thin-section analysis. Because large faults grow from smaller faults and because there are many more small faults than large faults, it is important to determine if the scaling relations are different for small and large faults. In this paper, we present the geometry and scaling relations of a population of exceptionally well exposed, small ($L < 1.25$ m) normal faults within a Mesozoic rift basin, and briefly discuss their relations to larger fault systems.

FAULT GEOMETRY AND SCALING RELATIONS

The small normal faults are present in quarries of the Virginia Solite Corporation located in the Mesozoic Dan River rift basin (Fig. 1). This basin is a northeast-trending, highly elongate half graben bounded on its northwestern margin by a moderately southeast-dipping border fault; strata within the basin dip to the northwest (Schlische, 1993). The small faults occur within gray siltstones of the Cow Branch Formation.

The small faults are best observed on bedding-plane surfaces of both in situ outcrops and quarried boulders (Fig. 2). The fault traces are typically straight, although the fault tips may be curved in the vicinity of larger faults. The faults exhibit a strong preferred orientation: they strike ~N40°E, which is parallel to the border fault of the basin and subparallel to bedding-perpendicular veins found in sandstone units. The faults and veins formed semicoevally in the different units in response to the same applied stress (Ackermann et al., 1996). The faults all dip moderately to the southeast; the fault-bedding angle is 70°–85°, suggesting that the faults originated at steep dips and were rotated to their present moderate dip through tilting of the beds. In cross section, the partially mineralized fault traces are observed to terminate upward and downward into zero-displacement cracks. Some fault planes contain tool and groove slickensides or fibrous slickensides (Fig. 2b). The slickenlines rake at high angles, indi-

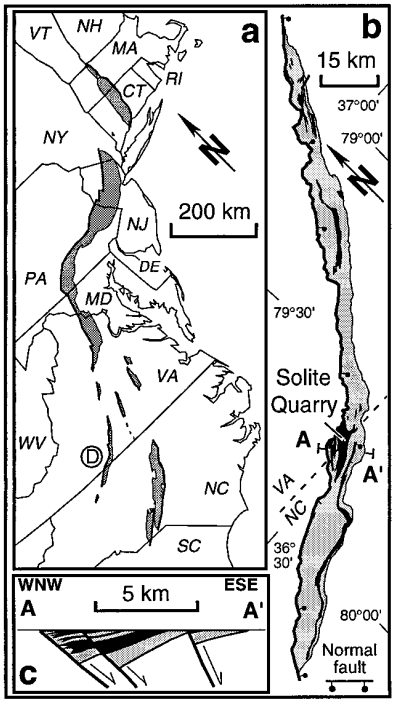

Figure 1. a: Exposed Mesozoic rift basins of eastern United States. D = Dan River basin. b: Simplified geologic map of Dan River basin, showing location of study area (Solite Quarry). Black represents Cow Branch Formation; other lithologic units not differentiated. c: Simplified geologic cross section of Dan River basin (see b for location), illustrating half-graben geometry. Modified from Schlische (1993).

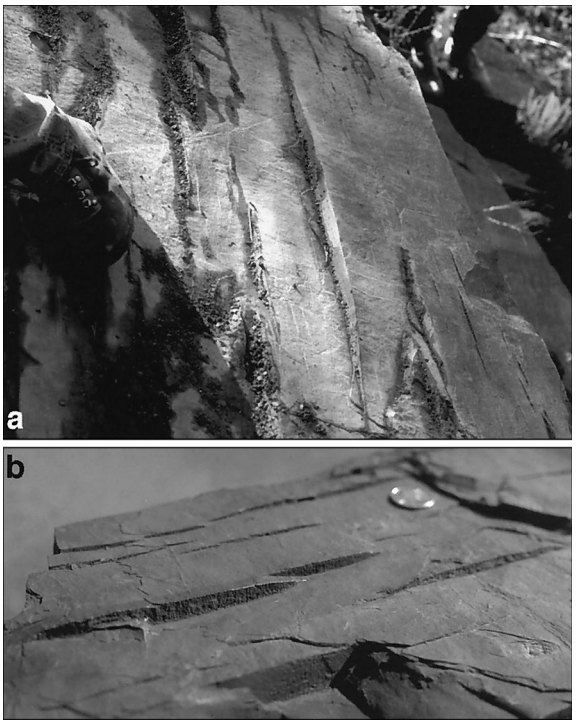

Figure 2. a: Photograph of in situ normal faults offsetting exposed bedding surface. Note that faults are all parallel to one another. Large fault at center has trace length of 123.1 cm and maximum observed displacement of 4.3 cm. Displacement is greatest at center of fault and decreases toward fault tips. b: Photograph of top surface of quarried slab showing slickensided faults. Note relay ramp between two largest faults. Dime (1.8 cm) for scale.

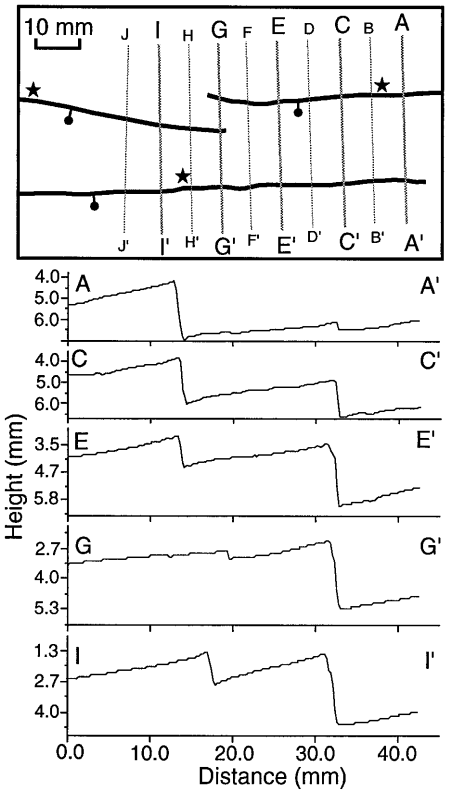

Figure 3. Top: Map of bedding surface cut by three normal faults. Stars indicate approximate locations of maximum observed displacement. Shaded lines show location of profiles along which deflection of bedding surface was measured with profilometer. Bottom: Bedding deflection profiles obtained from profilometer. Vertical axis is distance below some datum; horizontal axis is distance along profile line. Note upwarping in footwall and downwarping of hanging wall immediately adjacent to faults, which is manifestation of reverse drag.

cating predominantly dip-slip faulting. The preferred orientation of the faults and the presence of mineralization indicate that the faults are tectonic features.

The small faults occur both as isolated features (Fig. 2a) and as linked fault systems (Fig. 2b). Isolated fault surfaces are approximately elliptical, on the basis of direct observation of complete fault surfaces as well as serial sectioning (Gupta and Scholz, 1996). In linked faults, relay ramps are present between the overlapping fault segments. Relay structures are common to faults at a variety of scales (e.g., Peacock and Sanderson, 1991).

The faults exhibit normal-sense offset of bedding surfaces (Fig. 2), which generally can be traced continuously from the footwall to the hanging wall around the fault tips. Bedding surfaces in the vicinity of the faults are flexed downward in the hanging wall—defining a scoop-shaped depression (Gupta and Scholz, 1996) indistinguishable in geometry from half-graben basins (e.g., Schlische, 1993)—and upward in the footwall. In many instances, footwall uplift is equal to or greater than hanging-wall subsidence. Isostasy is primarily thought to be responsible for footwall uplift for large faults (e.g., Jackson and McKenzie, 1983), but clearly is unimportant for these small faults.

Fault displacements recorded by offset bedding surfaces were measured utilizing specially constructed microrulers and a profilometer. The smallest measurable displacement using the microruler is 0.02 cm. Displacement profiles were measured as scarp height versus distance along the scarp; this approach is justified because the slickenlines rake steeply. The profilometer (see Brown and Scholz, 1985) measures the topography of a surface by determining the distance from some reference level to the surface, which in this case is the faulted bedding surface. The instrument can detect elevation changes as small as 2 μm. Serial profiles obtained normal to three small normal faults (Fig. 3) indicate that displacement varies along the length of the faults. The profiles also show that bedding deflection decreases away from the fault in both the hanging wall and footwall. The deflection (reverse drag) is a manifestation of a decrease in displacement away from the fault and is not related to listric faulting. Deflection geometry is broadly consistent with elastic models (Gupta and Scholz, 1996), although the close proximity of two of the faults influences the magnitude and sign of the deflection.

Displacement is generally greatest at or near the center of the fault and decreases toward the fault tips. In many cases, displacement profiles resemble bell-shaped curves (Fig. 4b); this geometry is predicted by Cowie and Scholz's (1992b) model of faulting involving a process zone at the fault tips. In other cases, the displacement profiles exhibit flat-topped central portions and more steeply sloping distal portions (Fig. 4, a and c). Somewhat more complicated geometries arise for linked faults (Fig. 4c). The region of maximum displacement may be

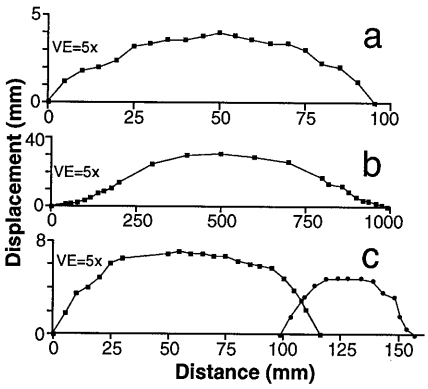

Figure 4. Displacement vs. distance plots for two isolated normal faults (a and b) and linked fault system (c). Note that displacement gradients are higher at tips of linked faults. VE = vertical exaggeration.

offset from the center of the fault segment; displacement gradients are higher in the vicinity of the overlapping fault tips. All measured displacement profiles are similar to

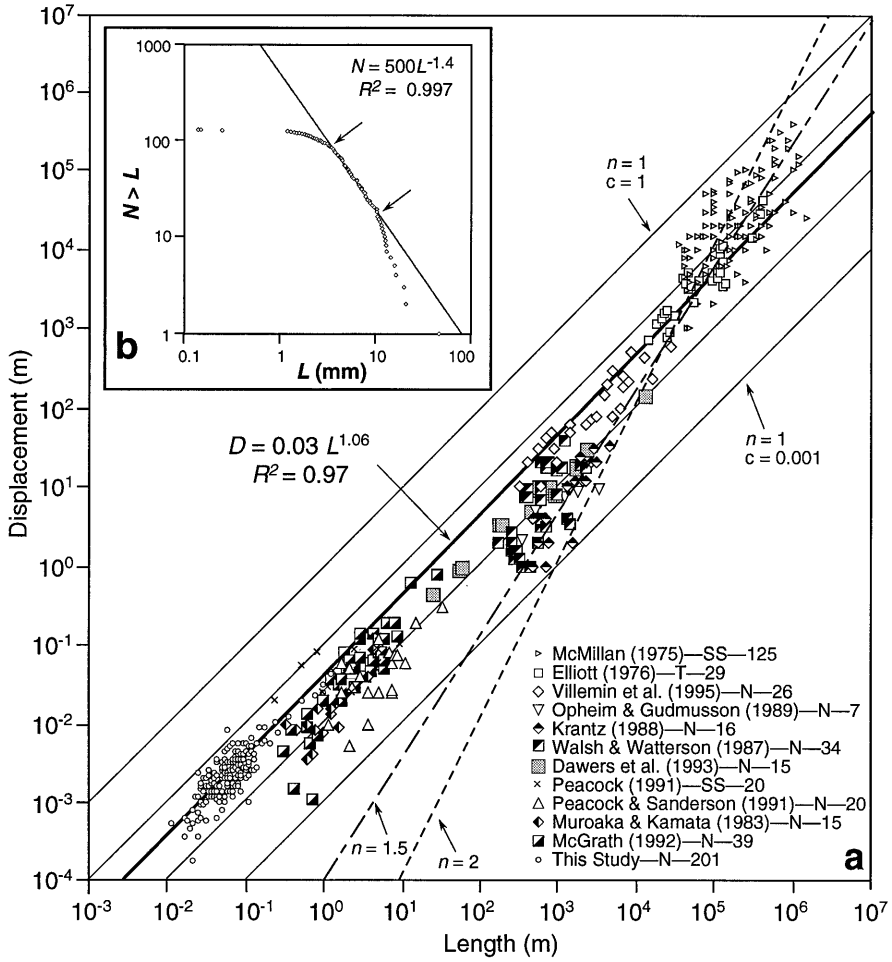

Figure 5. a: Log-log plot of displacement vs. length for various published fault populations as well as Solite data set. Abbreviations: N, normal faults; T, thrust faults; SS, strike-slip faults. Family of linear curves (n = 1) with various c values bound data; best-fit curve for all data is shown as heavy solid line. Also shown for reference are curves for n = 1.5 and n = 2. b: Size distribution of trace lengths of all faults from two-dimensional sampling of bedding surface on quarried boulder. Arrows delimit data points used to determine power-law exponent (1.4) for power-law distribution.

those of larger faults (e.g., Dawers et al., 1993). Furthermore, there are no significant differences in displacement geometry for small and large versions of the normal faults discussed here.

Trace lengths (tip-to-tip straight-line distance) and displacements were obtained for 201 normal faults from the Solite Quarry (Fig. 5a). Only those faults offsetting "clean" bedding surfaces that could be traced continuously from the footwall to the hanging-wall block are included. In addition, only isolated faults and hard-linked faults that kinematically behave like isolated faults are included. Soft-linked faults (overlapping faults separated by relay ramps) were excluded, given the uncertainty of defining trace length (segment length versus combined length) and maximum displacement (maximum displacement per segment versus maximum summed displacement) for fault systems in various stages of linkage. Because soft-linked faults represent an intermediate evolutionary stage between isolated faults and hard-linked faults that behave like isolated faults, we consider faults from these latter two end members to be sufficient to constrain the D-L scaling relation.

The data span just over two orders of magnitude for length (1.15 cm to 123.3 cm) and displacement (0.018 cm to 4.3 cm). The maximum observed displacement may be less than the true maximum displacement on a particular fault if the offset bedding surface did not intersect the center of the fault; the same caveat applies to trace length. The best-fit linear curve for the Solite data set has a slope (D/L ratio) of 0.030; the correlation coefficient, R^2, is 0.916. Correlation coefficients for power-law and exponential fits are 0.724 and 0.44, respectively. The best-fit power-law curve has a power-law exponent of 0.914, which is nearly linear.

The size distribution of faults for one bedding surface (measuring 50 cm by 60 cm) is shown in Figure 5b. The data points lie along a curve that has three distinct segments, similar to other cumulative frequency plots (e.g., Pickering et al., 1995). The shallow upper part reflects data censoring resulting from detection limits; the lower steep part results from truncation effects (faults extending beyond the study area). The central linear part of the curve indicates a power-law distribution of fault sizes of the form $N = aL^{-S}$, where N is number, a is a constant, L is length, and S is the slope of the straight-line part of the curve (the power-law exponent) and corresponds to the fractal dimension for two-dimensional sampling, which in this case is 1.4. This value is somewhat larger than that determined for the population of fault lengths (two-dimensional sampling) studied by Scholz and Cowie (1990). Higher values of S for a given sampling dimension indicate that smaller faults are increasingly important in accommodating strain (Marrett and Allmendinger, 1991).

DISCUSSION

As noted in the introduction, the value of n in the scaling relation $D = cL^n$ has been the topic of much attention in the literature. The Solite data (Fig. 5a) indicate a linear relationship between D and L, and therefore $n = 1$. A linear scaling relation between D and L has also been noted for larger faults (Elliott, 1976; Opheim and Gudmundson, 1989; Dawers et al., 1993; Carter and Winter, 1995; Villemin et al., 1995). However, most of the data sets shown in Figure 5a exhibit considerable scatter, making determinations of n difficult (Cowie and Scholz, 1992a; Gillespie et al., 1992).

Potential sources of the scatter include measurement errors, sampling of faults in different lithologies, effects of fault linkage (Cartwright et al., 1995), and not measuring maximum fault length and maximum displacement (e.g., Gillespie et al., 1992). With regard to the Solite data set, measurement error is considered to be very small given the complete exposure of the faults. Lithologic effects are also minimal because all faults were measured in the same type of rock (siltstones). The effects of linkage on scatter are small because faults that are obviously linked via relay ramps were not measured; however, some scatter may reflect measured faults that consist of multiple fault segments that grew together in the same plane and have not completely linked together. Some scatter is also due to the fact that maximum displacements and maximum lengths were not always measured.

With the exception of the data sets of Dawers et al. (1993), Carter and Winter (1995), and the Solite Quarry, the various

fault populations span less than two orders of magnitude of length, which, given the large scatter in the data, may make determinations of n problematic (Cowie and Scholz, 1992a; Gillespie et al., 1992). In part to overcome this difficulty, several workers have combined data sets and concluded that $n \approx 2$ (Watterson, 1986; Walsh and Watterson, 1988) or $n \approx 1.5$ (Marrett and Allmendinger, 1991; Gillespie et al., 1992). However, Cowie and Scholz (1992a) argued that faults from different lithologies and tectonic environments will likely have different c values and thus should not be combined. Nonetheless, visual inspection of the global data set (Fig. 5a) indicates that it is most consistent with a linear scaling relationship between displacement and length. The data lie between linear curves with c values ranging from 1 to 0.001. The best fit curve for the global data set is given by the equation $D = 0.03L^{1.06}$, which is also virtually linear. Note that the $n = 2$ and $n = 1.5$ curves shown in Figure 5a significantly underestimate displacements for faults in the length range present in the Solite Quarry.

The global data set indicates that there is no significant change in the *D-L* scaling relation over the more than eight orders of magnitude of fault length shown in Figure 5a: the global data set exhibits linear *D-L* scaling, as do most of the individual data sets. There does, however, appear to be change in the value of c that occurs at $L = \sim 1000$ m, smaller faults generally having somewhat lower values of c than larger faults. Presumably, larger faults sample deeper, and thus stronger, rocks that have higher c values (Cowie and Scholz, 1992a). Thus, other than the c value, which is a function of rock properties and tectonic environment, there is no difference between "small" and "large" faults. Furthermore, the scaling law and the deformation mechanism responsible for it do not break down at very small scales and presumably lower values of finite strain. The linear relation between L and D for the Solite data support Cowie and Scholz's (1992b) elastic-plastic fault-growth model.

In summary, the very small normal faults present in the Solite Quarry represent an important new fault population data set: it spans more than two orders of magnitude, is the largest data set to date, contains faults confined to a single lithology, and covers a range of lengths and displacements not previously studied; furthermore, the faults are completely exposed over their entire lengths. The very small Solite faults share many of the same characteristics of larger faults, including displacement geometry, footwall uplift, style of fault linkage, and a power-law distribution of fault sizes. These very small faults indicate that the scaling relation between length and displacement is linear, is not perceptibly different for small and large faults, and does not break down for very small faults. Given these similarities, such exceptionally well exposed very small faults provide an opportunity to study aspects of faulting and fault growth that are not possible for larger faults, including mapping three-dimensional displacement geometries (Gupta and Scholz, 1996) and examining the spatial distribution of faults (Ackermann et al., 1995).

ACKNOWLEDGMENTS

Research was supported by grants from the Henry Rutgers Scholars Program to Young, the Rutgers University Research Council and the Virginia Museum of Natural History to Schlische, and National Science Foundation (grant EAR 93-05175) to C. Scholz and M. Anders. We are grateful to the owners and employees of the Solite Quarry, especially C. H. Gover, for permitting access to the quarry and for providing logistical support. P. Olsen, B. Shaw, and N. Dawers provided valuable insights and field assistance. A. McGrath provided unpublished data. We thank R. Allmendinger, M. Carr, P. Cowie, N. Dawers, P. Rona, C. Scholz, and B. Trudgill for reviewing the manuscript.

REFERENCES CITED

Ackermann, R. V., Schlische, R. W., and Young, S. S., 1995, Anti-clustering of microfaults around larger normal faults: Differential strain accommodation in the Danville basin: Eos (Transactions, American Geophysical Union), v. 76, no. 46 (supplement), p. F-574.

Ackermann, R. V., Johnson, L. A., Patino, L. C., and Schlische, R. W., 1996, Fracture partitioning in the Cow Branch Formation, Danville rift basin: Influence of mechanical stratigraphy on Mohr-Coulomb failure: Geological Society of America Abstracts with Programs, v. 28, no. 3, p. 33.

Brown, S. R., and Scholz, C. H., 1985, Broad bandwidth study of the topography of natural rock surfaces: Journal of Geophysical Research, v. 90, p. 12575–12582.

Carter, K. E., and Winter, C. L., 1995, Fractal nature and scaling of normal faults in the Española Basin, Rio Grande rift, New Mexico: Implications for fault growth and brittle strain: Journal of Structural Geology, v. 17, p. 863–873.

Cartwright, J. A., Trudgill, B. D., and Mansfield, C. S., 1995, Fault growth by segment linkage: An explanation for scatter in maximum displacement and trace length data from the Canyonlands Grabens of SE Utah: Journal of Structural Geology, v. 17, p. 1319–1326.

Cowie, P. A., and Scholz, C. H., 1992a, Displacement-length scaling relationship for faults: Data synthesis and discussion: Journal of Structural Geology, v. 14, p. 1149–1156.

Cowie, P. A., and Scholz, C. H., 1992b, Physical explanation for displacement-length relationship of faults using a post-yield fracture mechanics model: Journal of Structural Geology, v. 14, p. 1133–1148.

Dawers, N. H., Anders, M. H., and Scholz, C. H., 1993, Fault length and displacement: Scaling laws: Geology, v. 21, p. 1107–1110.

Elliott, D., 1976, Energy balance and deformation mechanisms of thrust sheets: Royal Society of London Philosophical Transactions, Ser. A, v. 283, p. 289–312.

Gillespie, P. A., Walsh, J. J., and Watterson, J., 1992, Limitations of dimension and displacement data from single faults and the consequences for data analysis and interpretation: Journal of Structural Geology, v. 14, p. 1157–1172.

Gupta, A., and Scholz, C. H., 1996, Three-dimensional geometry of small normal faults: Geological Society of America Abstracts with Programs, v. 28, no. 3, p. 60–61.

Jackson, J., and McKenzie, D., 1983, The geometrical evolution of normal fault systems: Journal of Structural Geology, v. 5, p. 471–482.

Krantz, R. W., 1988, Multiple fault sets and three-dimensional strain: Journal of Structural Geology, v. 10, p. 225–237.

Marrett, R., and Allmendinger, R. W., 1991, Estimates of strain due to brittle faulting: Sampling of fault populations: Journal of Structural Geology, v. 13, p. 735–738.

McGrath, A., 1992, Fault propagation and growth; a study of the Triassic and Jurassic from Watchet and Kilve, North Somerset [Master's thesis]: London, Royal Holloway, University of London, 165 p.

McMillan, R. A., 1975, The orientation and sense of displacement of strike-slip faults in continental crust [Bachelor's thesis]: Ottawa, Ontario, Carleton University.

Muraoka, H., and Kamata, H., 1983, Displacement distribution along minor fault traces: Journal of Structural Geology, v. 5, p. 483–495.

Nicol, A., Walsh, J. J., Watterson, J., and Gillespie, P. A., 1996, Fault size distributions—Are they really power-law?: Journal of Structural Geology, v. 18, p. 191–197.

Opheim, J. A., and Gudmundsson, A., 1989, Formation and geometry of fractures, and related volcanism, of the Krafla fissure swarm, northeast Iceland: Geological Society of America Bulletin, v. 101, p. 1608–1622.

Peacock, D. C. P., 1991, Displacements and segment linkage in strike-slip fault zones: Journal of Structural Geology, v. 13, p. 1025–1035.

Peacock, D. C. P., and Sanderson, D. J., 1991, Displacements, segment linkage and relay ramps in normal fault zones: Journal of Structural Geology, v. 13, p. 721–733.

Pickering, G., Bull, J. M., and Sanderson, D. J., 1995, Sampling power-law distributions: Tectonophysics, v. 248, p. 1–20.

Schlische, R. W., 1993, Anatomy and evolution of the Triassic-Jurassic continental rift system, eastern North America: Tectonics, v. 12, p. 1026–1042.

Scholz, C. H., and Cowie, P. A., 1990, Determination of total strain from faulting using slip measurements: Nature, v. 346, p. 837–838.

Villemin, T., Angelier, J., and Sunwoo, C., 1995, Fractal distribution of fault length and offsets: Implications of brittle deformation evaluation—Lorraine Coal Basin, *in* Barton, C. C., and La Pointe, P. R., eds., Fractals in the earth sciences: New York, Plenum Press, p. 205–226.

Walsh, J. J., and Watterson, J., 1988, Analysis of the relationship between displacements and dimensions of faults: Journal of Structural Geology, v. 10, p. 239–247.

Watterson, J., 1986, Fault dimensions, displacement, and growth: Pure and Applied Geophysics, v. 124, p. 365–373.

Manuscript received December 4, 1995
Revised manuscript received April 18, 1996
Manuscript accepted April 29, 1996